Available online at www.sciencedirect.com
ScienceDirect
Geochimica et Cosmochimica Acta 73 (2009) 2332–2346
Geochimica et Cosmochimica Acta
www.elsevier.com/locate/gca

Evidence for ocean acidification in the Great Barrier Reef of Australia

Gangjian Wei [a,b,*], Malcolm T. McCulloch [a,*], Graham Mortimer [a], Wengfeng Deng [b], Luhua Xie [b]

[a] *Research School of Earth Sciences, The Australian National University, Canberra, ACT 0200, Australia*
[b] *Key Laboratory of Isotope Geochronology and Geochemistry, Guangzhou Institute of Geochemistry, Chinese Academy of Sciences, Guangzhou 510640, China*

Received 27 May 2008; accepted in revised form 11 February 2009; available online 20 February 2009

Abstract

Geochemical records preserved in the long-lived carbonate skeleton of corals provide one of the few means to reconstruct changes in seawater pH since the commencement of the industrial era. This information is important in not only determining the response of the surface oceans to ocean acidification from enhanced uptake of CO_2, but also to better understand the effects of ocean acidification on carbonate secreting organisms such as corals, whose ability to calcify is highly pH dependent. Here we report an ~200 year $\delta^{11}B$ isotopic record, extracted from a long-lived *Porites* coral from the central Great Barrier Reef of Australia. This record covering the period from 1800 to 2004 was sampled at yearly increments from 1940 to the present and 5-year increments prior to 1940. The $\delta^{11}B$ isotopic compositions reflect variations in seawater pH, and the $\delta^{13}C$ changes in the carbon composition of surface water due to fossil fuel burning over this period. In addition complementary Ba/Ca, $\delta^{18}O$ and Mg/Ca data was obtained providing proxies for terrestrial runoff, salinity and temperature changes over the past 200 years in this region. Positive thermal ionization mass spectrometry (PTIMS) method was utilized in order to enable the highest precision and most accurate measurements of $\delta^{11}B$ values. The internal precision and reproducibility for $\delta^{11}B$ of our measurements are better than $\pm 0.2‰$ (2σ), which translates to a precision of better than ± 0.02 pH units. Our results indicate that the long-term pre-industrial variation of seawater pH in this region is partially related to the decadal–interdecadal variability of atmospheric and oceanic anomalies in the Pacific. In the periods around 1940 and 1998 there are also rapid oscillations in $\delta^{11}B$ compositions equivalent changes in pH of almost 0.5 U. The 1998 oscillation is co-incident with a major coral bleaching event indicating the sensitivity of skeletal $\delta^{11}B$ compositions to loss of zooxanthellate symbionts. Importantly, from the 1940s to the present-day, there is a general overall trend of ocean acidification with pH decreasing by about 0.2–0.3 U, the range being dependent on the value assumed for the fractionation factor $\alpha_{(B3-B4)}$ of the boric acid and borate species in seawater. Correlations of $\delta^{11}B$ with $\delta^{13}C$ during this interval indicate that the increasing trend towards ocean acidification over the past 60 years in this region is the result of enhanced dissolution of CO_2 in surface waters from the rapidly increasing levels of atmospheric CO_2, mainly from fossil fuel burning. This suggests that the increased levels of anthropogenic CO_2 in atmosphere has already caused a significant trend towards acidification in the oceans during the past decades. Observations of surprisingly large decreases in pH across important carbonate producing regions, such as the Great Barrier Reef of Australia, raise serious concerns about the impact of Greenhouse gas emissions on coral calcification.

1. INTRODUCTION

Ocean acidification from rapidly increasing anthropogenic CO_2 emissions has the potential to threaten marine

* Corresponding authors. Fax: +86 20 85290130 (G. Wei).
E-mail addresses: gjwei@gig.ac.cn (G. Wei), Malcolm.McCulloch@anu.edu.au (M.T. McCulloch).

0016-7037/$ - see front matter © 2009 Elsevier Ltd. All rights reserved.
doi:10.1016/j.gca.2009.02.009

ecosystems on a global scale. Atmospheric CO_2 concentrations are approaching 390 ppm, far beyond the 'natural' range of 200–280 ppm present during the past 400 kyr of glacial/interglacial cycles, and are continuing to increase at an accelerating rate of >2 ppm/yr. About 30–40 percent of the CO_2 injected into the atmosphere over the last century has been taken-up by the oceans (Orr et al., 2001), with a resultant increase in the hydrogen ion concentration $[H^+]$ of seawater, causing a reduction in seawater pH and trend towards ocean acidification (Caldeira and Wickett, 2003). Model calculations indicate that the increased levels of atmospheric CO_2 relative to the pre-industrial era has already caused an overall decrease of global seawater pH of 0.1 U, and further pH reduction of 0.2–0.3 are predicted for the next century (Caldeira and Wickett, 2003; Haugan and Drange, 1996) as discussed in the Fourth Assessment Report of IPCC (Intergovernmental Panel on Climate Change, 2007). Ocean acidification will reduce the level of carbonate saturation in seawater (Feely et al., 2004; Morse et al., 2006; Orr et al., 2005) and lead to reductions in rates of calcification (e.g. Langdon and Atkinson, 2005). If ocean acidification continues on its present trajectory, $CaCO_3$ dissolution will become more serious, as aragonite unsaturation is approached. As a result, some key marine calcareous organisms, such as calcareous micro-organisms and corals, will have difficulty to maintain their external carbonate skeletons (Kleypas et al., 1999; Hoegh-Guldberg et al., 2007; Miles et al., 2007; Roberts et al., 2006). In particular, coral reefs will be at great risk as coral calcification appears to be extremely sensitive to the level of carbonate saturation (Langdon and Atkinson, 2005).

Unfortunately, very little is known about the regional variability of ocean acidification on decadal to centennial time-scales, especially since the industrial era. Our current knowledge of ocean acidification is mainly the result of model calculations (Kleypas et al., 1999; Cao and Caldeira, 2008) and unlike other key climatic indices, such as temperature and salinity, until recently, seawater pH has seldom been recorded in marine observations due to the non-routine nature of the measurements. Accordingly, long-term continuous seawater pH records are scarce, with records now only approaching several decades from the offshore sites of Hawaii (Hawaii Ocean Time-series: HOT, see http://hahana.soest.hawaii.edu/hot/hot_jgofs.html) and Bermuda (Bermuda Atlantic Time-series Study: BATS, see http://bats.bios.edu/). This raises questions of how regional controls on seawater pH operate and what processes influence the variation of seawater pH over decadal to centennial time-scales. This lack of knowledge hinders attempts to properly evaluate not only the current status of ocean acidification, but importantly future trends and likely impacts on marine biota.

Boron isotopic systematics in marine carbonate provides a proxy for seawater pH as there is an isotopic fractionation between the boric acid, $B(OH)_3$ and borate ion, $B(OH)_4^-$ species in seawater (Kakihana et al., 1977), with the relative proportions of these species being controlled by pH (Hershey et al., 1986). Furthermore, only the $B(OH)_4^-$ species is incorporated into marine carbonate (Vengosh et al., 1991), hence the boron isotope composition in carbonate is a function of the ambient seawater pH during calcification (Hemming and Hanson, 1992; Vengosh et al., 1991). Some studies, however, argued that some observed high $^{11}B/^{10}B$ ratios in corals might indicate partial incorporation of $B(OH)_3$ into coral skeletons, potentially compromising the utility of coral boron isotopes as a seawater pH indicator (Xiao et al., 2006). Taking account of the calcification mechanism in corals at the cellular scale (Gattuso et al., 1999), the boron isotopic composition of coral skeletons reflect those of the internal fluid called extracytoplasmic calcifying fluid (ECF), which underlies the calicoblastic epithelium, or lowest tissue layer of the coral polyp cells where calcification takes place (Honisch et al., 2004). The ECF is separated from the ambient seawater by the coral polyp cells. It is generally postulated that Ca-ATPase enzymes work to transport protons, generated during calcification, away from the ECF to maintain high pH and transplant Ca^{2+} to the site of calcification at the same time for calcification (Al-Horani et al., 2003a; Gattuso et al., 1999; McConnaughey and Whelan, 1997). The on-going process of H^+ generation and removal results in larger pH variation in the ECF compared to that in ambient seawater (Al-Horani et al., 2003a; Hemming et al., 1998; Kuhl et al., 1995). Moreover, very little is known about the mechanism for boron transportation to the ECF from ambient seawater. Which species, $B(OH)_3$ or $B(HO)_4^-$, is preferentially transported, how they penetrate the polyp cells to reach ECF, and the boron speciation within the ECF, remain largely unknown. All of these factors can potentially complicate the relationship between coral skeletal boron systematics and ambient seawater pH. Fortunately, calibrations undertaken under controlled conditions using cultured biogenic carbonate, such as foraminifers (Sanyal et al., 2001) and corals (Honisch et al., 2004), indicates that the boron isotope composition in carbonates actively responds to changes of the ambient seawater pH, implying that boron isotope compositions in biogenic carbonate reliably reflect the changes in seawater pH, notwithstanding the uncertainties in calibration and species effects discussed below.

Most of the studies of boron isotope systematics in carbonates have focused on reconstructing paleoseawater pH in longer time-scales, such as glacial/interglacial cycles (10^5 years) or longer (10^6 years) through the early Cenozoic (Honisch et al., 2004; Honisch and Hemming, 2005; Pearson and Palmer, 1999; Sanyal et al., 1997; Sanyal et al., 1995), in which the pH records are used to infer levels of atmospheric pCO_2. To date very few studies have focused on the recent decadal to centennial pH record, which is the appropriate timescale for studying the effects of ocean acidification driven by anthropogenic emissions of CO_2. An exception is a pH record covering the past 300 years produced by the ANU laboratories at 5-yearly resolution using boron isotopic variations in a *Porites* coral from Flinders Reef in the Coral Sea, offshore of the East Australia (Pelejero et al., 2005). It is interesting to note that the variation of seawater pH in this region is mainly in response to the Interdecadal Pacific Oscillation (IPO) of ocean-atmosphere anomalies, with an ~50-year cycle in the past 300 years (Pelejero et al., 2005). However, due to these

oscillations there is no convincing evidence for a decrease in pH that can be unambiguously attributed to ocean acidification. This maybe due to the coral record ceasing in the mid 1980s, combined with the relatively large IPO oscillations. This indicates the importance of natural variability in seawater pH and that higher atmospheric CO_2 concentration will not necessarily result in a uniform reduction in seawater pH (Haugan and Drange, 1996). It is therefore apparent that the response of seawater pH to atmospheric CO_2 concentration is not a simple process, particularly in coral reef environments where coral calcification and photosynthesis can significantly perturb local pH. As recognized in the earlier study of Pelejero et al. (2005) more paleo-pH records covering the past several centuries at different locations and sufficient resolution are needed for a better understanding of how larger-scale ocean variations may interact with locally generated changes in pH produced within coral reef environments.

In order to reconstruct seawater pH variations over the past ~200 years (1800–2004) we have determined the boron isotopic variations at high temporal resolution from the carbonate skeleton of a long-lived *Porites* coral from the central Great Barriers Reef (GBR) of Australia. In contrast to the record of Pelejero et al. (2005), this coral is within the GBR and close to the Australian continent (~30 km). The time resolution of our record from 1940 to 2004 is at an annual resolution and at 5-yearly intervals prior to 1940, the latter being similar to the sample resolution of Pelejero et al. (2005). This new record provides insights into variation of seawater pH in a major near-shore coral reef at decadal to centennial time-scales. In addition to boron isotopes, Mg/Ca (proxy for sea surface temperature; SST), $\delta^{13}C$ (proxy for $\delta^{13}C$ of dissolved inorganic carbon; DIC), $\delta^{18}O$, and Ba/Ca (proxies for terrestrial input) are also reported. These geochemical records provide constraints on how seawater pH variation response is related to other climate/environment changes.

2. MATERIALS AND METHODS

A *Porites* sp. coral core was drilled in Arlington Reef, immediately offshore Cairns in the north-east coast of Australia in November 2004 (Fig. 1) using underwater drilling techniques and associated logistics developed at the Australian National University. The coral core was cut length-wise into 7-mm-thick slabs. Annual density bands where revealed by X-rays and occasional flood-plume related fluorescent lines by long-wave UV light and used to establish the chronology of the coral core. Generally, the highest density bands correspond to winter skeletal growth, and the fluorescent lines, when present, correspond closely with the summer period (January–February) when freshwater inputs from the coastal rivers are intensified by the Australian summer monsoon. The density and fluorescent chronologies agree well with each other and were independently verified by high resolution laser geochemistry.

The slabs were ultrasonically cleaned in water purified by Millipore system (MQ water), rinsed three times and dried at 40 °C prior to sampling. Before collecting the samples, preliminary milling along the designated sample track was undertaken to remove the upper ~1 mm surface. Fine powder was milled from 2 mm wide sampling grooves along the center of the maximum growth axis. The samples from 2004 to 1940 were milled in 1-year intervals, and in 5-year intervals from 1939 to 1800. For further details of the sampling method refer to Hendy et al. (2002) and Pelejero et al. (2005).

About 20 mg of fine powder was placed into a clean plastic tube, and then ~1 mL 30% H_2O_2 added and reacted with the coral powder for about two days. This step removes most of the organic matter inform the coral samples. The tube was then centrifuged and the supernatant removed. The remaining coral powder was then rinsed ×3 times with Milli-Q water. The coral sample was dissolved with ~0.2 mL 3 N HCl, and diluted to 1 mL with 0.1 N HCl.

A two-step column procedure was used to separate and purify the coral boron. The first column comprises ~0.5 mL of AG 50 × 8 cation resin filled in a 2 mL BioSpin column. The sample in 1 mL 0.1 N HCl was loaded onto the column directly. The sample was eluted with 2 mL (0.5 mL × 4) 0.1 N HCl and collected for further boron purification. The first column process removes the dominant Ca fraction that may form $Ca(OH)_2$ precipitates causing significant boron losses when increasing the pH during the subsequent step. Concentrated NH_4OH was then added until the pH value is >12. After allowing ~1 h for equilibrium, the solution was loaded onto the second B specific column, consisting of ~0.5 mL Amberlite IRA 743 resin in a 2 mL BioSpin column. Boron is quantitatively absorbed by the resin, and washed by eluting the column with ~0.03 M NH_4OH (repeated ×3 times) and 0.5 mL Milli-Q water. Boron was then eluted with 2.5 mL (0.5 mL × 5) 0.1 N HCl and collected. Some CsOH and mannitol were added into the B fraction to make the B/Cs and B/mannitol molar ratios at about a ratio of 1:2 and 3:4, respectively (Lemarchand et al., 2002), assuming that the boron concentration in coral samples is about 50 ppm. The solution was then dried under an infrared lamp at a temperature <60 °C in preparation for mass spectrometry.

The sample was loaded onto a degassed single Ta filament using 4 μL 0.1 N HCl, and dried under a lamp at <60 °C. Following the procedure of (Xiao et al., 1988), ~1 μL graphite suspension solution was added to the sample before it is completely dried, and the sample then immediately loaded into the mass spectrometer for boron isotope measurements.

Boron isotope compositions were measured on a Finnigan TRITON thermal ionization mass spectrometry (TIMS) in the Research School of Earth Sciences at the Australian National University. Positive ions with masses at 309 ($^{133}Cs^{133}Cs^{11}B^{16}O^{16}O + {}^{133}Cs^{133}Cs^{10}B^{16}O^{17}O)^+$ and 308 ($^{133}Cs^{133}Cs^{10}B^{16}O^{16}O)^+$ were measured at high mass in order to reduce the amount of instrumental-induced mass fractionation (Spivack and Edmond, 1986). The boron isotope ratio $^{11}B/^{10}B$ can be calculated from the ratio of $^{309}M/^{308}M$ with an ^{17}O correction (Spivack and Edmond, 1986) of:

$$^{11}B/^{10}B = {}^{309}M/^{308}M\text{-}0.00078$$

Boron isotope compositions are expressed as $\delta^{11}B$:

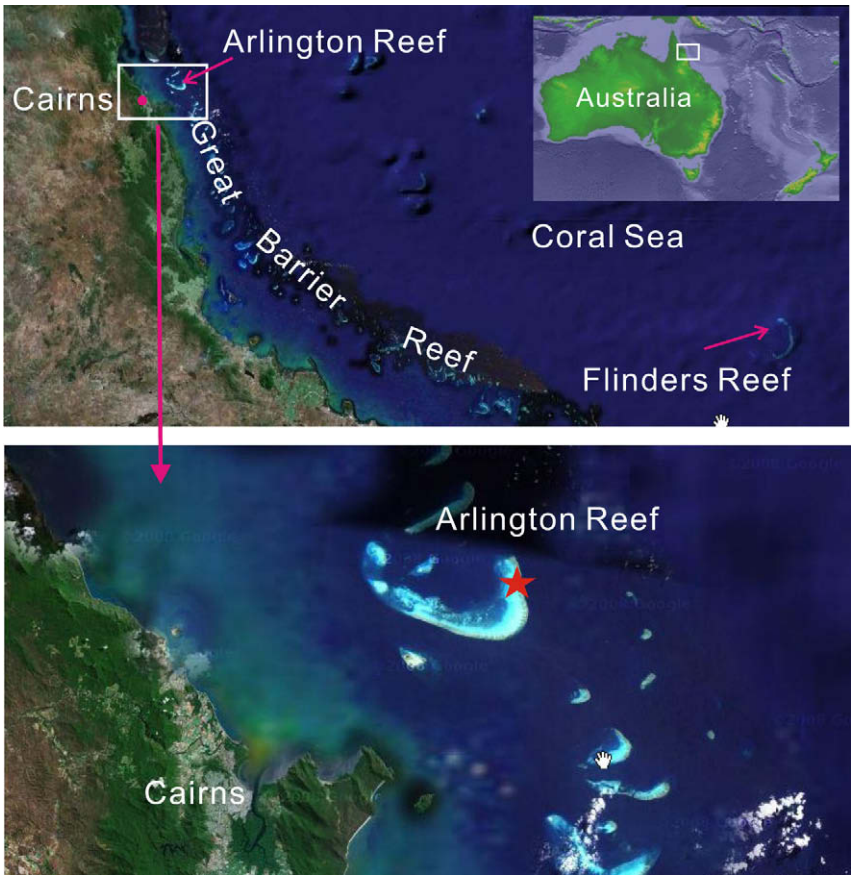

Fig. 1. Map showing the location of Arlington Reef in the Great Barrier Reef (GBR) and Flinders Reef in the Coral Sea. Dashed lines indicate the main coral reefs within the GBR. Insert shows location of the Great Barrier Reef of Northern Queensland.

$$\delta^{11}B = \left[\left(^{11}B/^{10}B\right)_{sample}/\left(^{11}B/^{10}B\right)_{standard} - 1\right] \times 1000$$

relative to the NIST SRM 951 standard.

Since the RSES TRITON center cup cannot exceed mass 300, the higher faraday cup H3 was adjusted to measure masses 308 and 309 when the center cup was positioned at masses 295 and 296, respectively. Simultaneously, the H2 cup was adjusted to measure mass 301 $(^{133}Cs^{133}Cs^{35}Cl)^+$ with the H3 cup at mass of 309. The ratio of 309/308 was measured in dynamic mode using H3 with 308 intensities in the range 50–100 mv. Multi-collector measurements where not possible due to space limitations for adjacent cups at masses 308–309 despite the use of the zoom optics. Measurements for each sample consisted of four blocks, with each block containing 20–25 cycles. Such ratio measurement generally reached <0.01% internal 2σ precision for 309/308 ratios, corresponding to an error of better than ±0.0008 for $^{11}B/^{10}B$ ratio.

Fig. 2 shows the within-run variations and reproducibility of $^{11}B/^{10}B$ ratios for the boron isotope standard, SRM 951, which was loaded directly onto a Ta filament without any chemical treatments. Fig. 2 shows no detectable $^{11}B/^{10}B$ ratio drift within a single measurement, and the reproducibility of different measurements is excellent, indicating that mass fractionation between 308 and 309 from different filament loads and during mass spectrometry measurement is insignificant.

In contrast when measuring coral samples there is generally an increasing trend in the $^{11}B/^{10}B$ ratio (Fig. 3a), which is attributed to isobaric interference of $(^{133}Cs^{133}Cs^{12}C^{14}N^{16}O)^+$ on $^{308}Cs_2BO_2^+$. The isobaric $^{308}Cs_2CNO^+$ interference is presumed to be from coral derived organic material despite the coral samples being treated with H_2O_2 before column chemistry. Some organic material apparently remains with the anomalously low 309/308 ratios attributed to

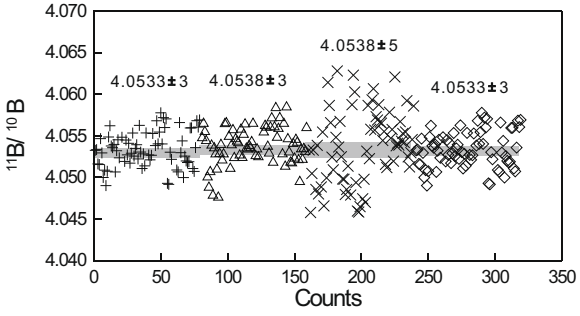

Fig. 2. Variations of $^{11}B/^{10}B$ ratios of SRM 987 during measurement using TRITON positive (P) TIMS. The $^{11}B/^{10}B$ ratios were calculated from the measured *m/e* 309/308 ratios using: $^{11}B/^{10}B = {}^{309}Cs_2BO_2^+/{}^{308}Cs_2BO_2^+$-0.00078. Symbols indicate the results from different filaments. The shaded bars indicate the average of the $^{11}B/^{10}B$ ratios for a single filament.

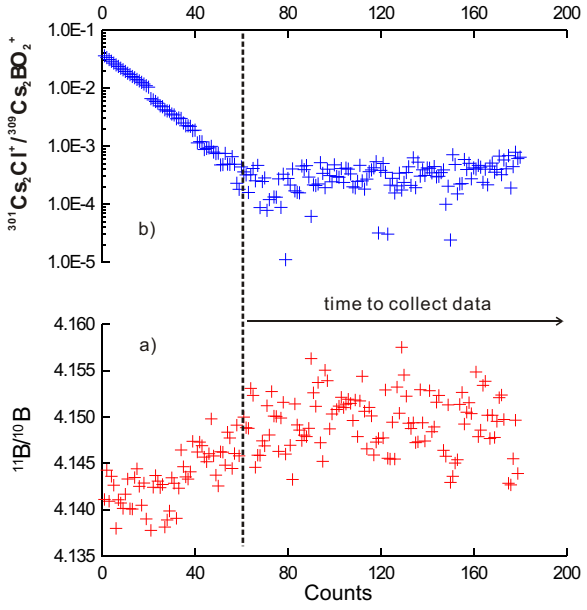

Fig. 3. Variations of $^{11}B/^{10}B$ and $^{301}Cs_2Cl^+/^{309}Cs_2BO_2^+$ ratios of a coral sample during measurement using PTIMS. (a) $^{11}B/^{10}B$ ratios as measured using $^{309}Cs_2BO_2^+$ and $^{308}Cs_2BO_2^+$complexes. (b) Measured $^{301}Cs_2Cl^+/^{309}Cs_2BO_2^+$ ratios. The vertical dashed line marks the point of exhaustion of $^{301}Cs_2Cl^+$, indicating that $^{308}Cs_2CNO^+$ interference on the $^{11}B/^{10}B$ ratios derived from $^{309}Cs_2BO_2^+/^{308}Cs_2BO_2^+$ is insignificant.

$^{308}Cs_2CNO^+$ interference. Because organic matter is exhausted more quickly than $Cs_2BO_2^+$, during measurement, a gradual decreasing of $^{308}Cs_2CNO^+$ isobaric interference, produces an increase in 309/308 ratio. Interference free 309/308 data is therefore obtained from the plateau region shown in Fig. 3a, which occurs after the organic matters has decayed. Thus careful monitoring of interferences is essential for accurate $^{11}B/^{10}B$ ratios. Some studies suggest the addition of H_3PO_4 to the sample during filament loading (Wei et al., 2004). H_3PO_4 may retard the ionization of $Cs_2BO_2^+$, and help to exhaust organic interferences before data collection. However, the decay rate of $Cs_2BO_2^+$ signal increases at higher temperature and as a result, the $Cs_2BO_2^+$ signal generally cannot be sustained to obtain high-precision results necessary for this study.

Here we also use $^{301}Cs_2Cl^+$ to monitor $^{308}Cs_2CNO^+$. Like $^{308}Cs_2CNO^+$, $^{301}Cs_2Cl^+$ is more readily exhausted compared to $Cs_2BO_2^+$. As shown in Fig. 3b, the $^{301}Cs_2Cl^+/^{309}Cs_2BO_2^+$ ratio decreases rapidly at the early stage of measurement, concomitant with an increasing 309/308 ratio. When the $^{301}Cs_2Cl^+/^{309}Cs_2BO_2^+$ ratio decreases to a very low level, generally about 10^{-3}–10^{-4}, the ratio of 309/308 also reaches a plateau, indicating that the isobaric interference of $^{308}Cs_2CNO^+$ is insignificant and the $\delta^{11}B$ data is interference free. Using this method, the precision and reproducibility of $^{11}B/^{10}B$ for coral samples are comparable with those obtained for the SRM 951 standard.

In order to evaluate the influence of column chemistry on boron isotope ratios, SRM 951 solutions were also processed through the two-step column chemistry used for the coral samples. The $^{11}B/^{10}B$ ratios of the SRM 951 after such treatment show an average of 4.0542 ± 0.0005 ($n = 10$), which is the same as the long-term average of SRM 951 of 4.0540 ± 0.0003 without chemical processing. The $^{11}B/^{10}B$ results of SRM 951 after column chemistry are listed in Table 1. A modern *Porites* coral, collected at Davies Reef in the central Great Barrier Reefs, was used as a secondary working standard, and repeatedly measured with other coral samples. These results are also listed in Table 1, and the average $^{11}B/^{10}B$ of Davies Reef coral is 4.1558 ± 0.0004, corresponding to $\delta^{11}B = 25.12 \pm 0.11$ relative to the long-term average of SRM 951 (4.0540) measured on our machine. A seawater standard from the Great Barrier Reef was also analyzed giving a $\delta^{11}B$ value of 40.08 ± 0.08 (Table 1).

Acids and NH_4OH were prepared using distilled reagents, and H_2O_2 and mannitol used are in analytical grade form. The blank of all the reagents, including Milli-Q water, HCl, NH_4OH, and mannitol, as well as the blank of the whole chemical procedure and loading blank on Ta filament,

Table 1
Boron isotope composition of standard SRM 951, Davies Reef coral and seawater.

	$^{11}B/^{10}B$	2σ	$\delta^{11}B$[a]	2σ
Standard SRM 951 directly loaded on Ta filament				
Mean	4.0532	0.0003		
Standard SRM 951 processed through column chemistry				
1	4.0530	0.0006	−0.06	0.15
2	4.0535	0.0012	0.07	0.29
3	4.0536	0.0006	0.10	0.16
4	4.0520	0.0008	−0.30	0.20
5	4.0534	0.0004	0.06	0.10
6	4.0534	0.0006	0.05	0.14
7	4.0542	0.0005	0.24	0.12
8	4.0530	0.0006	−0.06	0.15
9	4.0535	0.0012	0.07	0.29
10	4.0538	0.0005	0.14	0.13
Mean	4.0534	0.0004	0.06	0.10
Working standard: Davies Reef coral				
1	4.1547	0.0009	24.84	0.22
2	4.1549	0.0013	24.90	0.32
3	4.1562	0.0008	25.21	0.19
4	4.1562	0.0008	25.20	0.19
5	4.1561	0.0006	25.18	0.13
6	4.1557	0.0005	25.09	0.12
7	4.1547	0.0007	24.84	0.17
8	4.1566	0.0003	25.31	0.07
9	4.1563	0.0005	25.24	0.12
10	4.1559	0.0003	25.14	0.07
11	4.1548	0.0005	24.87	0.12
12	4.1550	0.0004	24.92	0.10
Mean	4.1558	0.0004	25.12	0.11
Seawater				
1	4.2155	0.0003	40.05	0.07
2	4.2165	0.0003	40.32	0.08
3	4.2153	0.0002	40.02	0.05
4	4.2150	0.0002	39.95	0.05
Mean	4.2156	0.0002	40.08	0.08

[a] $\delta^{11}B = 1000 \times [(^{11}B/^{10}B)\text{sample}/(^{11}B/^{10}B)\text{standard} - 1]$, where $(^{11}B/^{10}B)$standard equals the long-term average of SRM 951 directly loaded on Ta filament, 4.0532.

have been tested using isotope dilution spiked with the ^{10}B SRM 952. The blanks were measured using negative ions of $^{42}BO_2^-$ and $^{43}BO_2^-$ (Pelejero et al., 2005), which is extremely sensitive to small boron signals. All of the blanks are at the level of 10^{-9} g. The coral sample size in our measurement is about 20 mg, equivalent to $\sim 10^{-6}$ g of boron and therefore, reagents and procedural blanks are insignificant. This is also supported by the consistency between the $^{11}B/^{10}B$ ratios of SRM 951 after column chemistry and those loaded directly.

Sr/Ca, Mg/Ca and Ba/Ca ratios of the coral samples were measured on a Varian Vista inductively coupled plasma atomic emission spectrometry (ICP-AES) in the Key Laboratory of Isotope Geochronology and Geochemistry of Chinese Academy of Sciences in Guangzhou Institute of Geochemistry. Details of the analytical methods are given by (Wei et al., 2007). Precision for Sr/Ca and Mg/Ca ratios is better than 0.3%, and about 1–3% for Ba/Ca ratios. Oxygen and carbon isotopes of the coral samples were measured on a GV Isoprime II isotope ratio mass spectrometry (IRMS) coupled with Dual Inlet® and Multiprep®, an online carbonate preparation system, in the same laboratory. The oxygen and carbon isotope compositions are expressed as $\delta^{18}O$ and $\delta^{13}C$ relative to Vienna PDB standard. Precision for oxygen and carbon isotopes are better than 0.08‰ (1σ) and 0.05‰ (1σ), respectively. These data, together with the boron isotope results, are listed in Table 2 and shown in Fig. 4.

3. RESULTS

The $\delta^{11}B$ values of the *Porites* coral from Arlington Reef ranges from 25.4‰ to 21.1‰. The maximum $\delta^{11}B$ value of 25.4‰ occurs in the 1857, representing a 5-year interval, and in the 1947 1-year sample, a similar value of 25.1‰ is obtained. The minimum $\delta^{11}B$ values (<22‰) occur during 1935–1940 also a 5-year sample and in the yearly samples at 1998 and 2004. Importantly from 1941 to 2004, there is an overall trend of decreasing coral $\delta^{11}B$ values (Fig. 4a).

The $\delta^{13}C$ of the coral varies relatively systematically from −0.98‰ to −3.56‰ with an overall decrease towards more negative $\delta^{13}C$ values for the period of 1850–2004 (Fig. 4b). However, the decrease during the most recent 50 years is especially significant, from ∼−1.4‰ in 1942 to ∼−3.6‰ in 2004, representing an overall shift of ∼−2‰.

The Mg/Ca ratios range from 3.5 to 4.5 mmol/mol. From 1800 to 1910, the Mg/Ca ratios decrease gradually, and increase for the period from 1950 to 2004 (Fig. 4c). Significant negative $\delta^{18}O$ peaks and positive Ba/Ca peaks are observed around the years 1840, 1880 and 1953 consistent with major river flood-plumes reaching the reef. The $\delta^{18}O$ show a slight decreasing trend after 1920, which is similar to that of the $\delta^{13}C$ and inverse to that of the Mg/Ca ratios.

4. DISCUSSION

4.1. Long-term variation of coral $\delta^{11}B$

The temporal variation of the $\delta^{11}B$ of the coral from Arlington Reef exhibits an overall decreasing trend since 1940 and obvious interdecadal fluctuations since 1800 as shown in Fig. 4. Such interdecadal fluctuations have also been observed in another coral $\delta^{11}B$ record in Flinders Reef in the adjacent region (Pelejero et al., 2005), which is the only other published long-term coral $\delta^{11}B$ record and also shows a relationship to the Interdecadal Pacific Oscillation (IPO) of ocean-atmosphere anomalies (Pelejero et al., 2005). The temporal variations of both coral $\delta^{11}B$ records, as well as the filtered IPO index, represented by the temperature anomalies during January-February-March (Folland et al., 1999; Power et al., 1999) are shown in Fig. 5. The coral $\delta^{11}B$ in Flinders Reef vary from 22.99‰ to 24.89‰, which is within the variation range for those in Arlington Reef, but the maximum fluctuation amplitude in the Flinders Reef record is only about half of that in the Arlington Reef record (Fig. 5). Even though not exactly in phase, the interdecadal fluctuations in the two coral $\delta^{11}B$ records appear to be partially related to the variation of the IPO index, in particular the rapid variations of coral $\delta^{11}B$ correspond to rapid IPO changes. For example, the rapid increase of $\delta^{11}B$ values around 1940 in the Arlington Reef record, approximately corresponds to the rapid shifting of the IPO index from its maximum positive value (∼1.7) in 1940 to its maximum negative value (∼−1.7) in 1951 (Fig. 5). It is noted, however, that there are also some inconsistencies with the IPO, in particular the high $\delta^{11}B$ values from 1993 to 1995 followed by the rapid fall in values centered at 1998, suggesting that other factors are also at play.

The interdecadal fluctuation of these coral $\delta^{11}B$ records from the Great Barrier Reef is further illustrated by their power spectra (Fig. 6), which were calculated using the software of REDFIT (Schulz and Mudelsee, 2002). A robust 48-year cycle is present in the Flinders Reef pH spectrum (Fig. 6a), and a robust 22- and 10-year cycles, which are significant at the 95% confident level, and a weak 50-year cycle, which is significant at the 80% confident level, are present in the Arlington Reef pH spectrum (Fig. 6b). These decadal–interdecadal cycles are the characteristic periodicities for the Pacific Decadal Oscillation (PDO) of Pacific climate variability (Mantua and Hare, 2002) or IPO (Folland et al., 1999; Power et al., 1999), and they are well represented in coral paleoclimate records covering the past several centuries in the Pacific and adjacent regions (Cobb et al., 2001; Linsley et al., 2000a; Linsley et al., 2000b; Sun et al., 2004). The difference of the periodicities shown by the two pH records may in part be attributed to the difference in age range and temporal resolution. The Flinders Reef record has longer time span, ∼300 years, but lower time resolution, in 5-year interval, while the Arlington Reef record covers a shorter time span from 1800 to 2004, but at higher resolution (1-year intervals) from 1940 to 2004. Therefore, the lower frequency (∼50-year) is readily apparent in the Flinders Reef record, whereas the higher frequencies (22-year and 10-year) are more apparent in the Arlington Reef record. Even though the periodicities represented are different, they may still be related to the PDO or IPO, indicating that the long-term variation of seawater pH in the west Pacific may response to the decadal–interdecadal climate variability in the Pacific on centennial time scale. However, the specific mechanisms for the linkage

Table 2
The analyzed and calculated data of AREO 4 coral.

Sample ID	Year[a]	Mg/Ca[b] ($\times10^{-3}$)	Sr/Ca[b] ($\times10^{-3}$)	Ba/Ca[b] ($\times10^{-6}$)	$\delta^{13}C$[c] (‰)	$\delta^{18}O$[c] (‰)	$\delta^{11}B$[d] (‰)	2σ	pH[e]	$2\sigma_{mean}$[e]
AREO 4 1805-09	1807	4.310	7.762	3.53	−1.59	−4.40	23.61	0.16	8.02	0.02
AREO 4 1810-14	1812	4.139	7.910	4.03	−2.00	−4.49	24.53	0.15	8.13	0.02
AREO 4 1815-19	1817	4.302	7.773	3.36	−1.47	−4.56	22.74	0.15	7.90	0.02
AREO 4 1820-24	1822	4.101	7.792	3.71	−1.25	−4.49	23.86	0.16	8.05	0.02
AREO 4 1825-29	1827	4.249	7.745	3.31	−1.36	−4.37	24.77	0.12	8.15	0.01
AREO 4 1830-34	1832	4.233	7.809	3.58	−1.22	−4.49	23.60	0.14	8.02	0.02
AREO 4 1835-39	1837	4.333	7.747	3.44	−1.26	−4.40	23.12	0.16	7.95	0.02
AREO 4 1840-44	1842	4.330	7.756	5.31	−1.46	−5.15	22.88	0.16	7.92	0.02
AREO 4 1845-49	1847	4.437	7.728	2.81	−0.99	−4.51	22.94	0.20	7.93	0.03
AREO 4 1850-54	1852	4.125	7.715	3.22	−1.03	−4.37	22.90	0.17	7.92	0.02
AREO 4 1855-59	1857	4.065	7.705	2.82	−0.99	−4.36	25.38	0.08	8.22	0.01
AREO 4 1860-64	1862	3.986	7.693	4.22	−0.98	−4.49	22.63	0.12	7.88	0.02
AREO 4 1865-69	1867	3.991	7.686	3.21	−1.06	−4.54	22.53	0.17	7.87	0.02
AREO 4 1870-74	1872	3.929	7.642	3.19	−1.49	−4.65	22.53	0.20	7.87	0.03
AREO 4 1875-79	1877	3.841	7.639	4.13	−1.08	−4.59	23.14	0.17	7.96	0.02
AREO 4 1880-84	1882	4.003	7.663	6.78	−1.29	−5.77	22.96	0.19	7.93	0.02
AREO 4 1885-89	1887	3.968	7.730	3.21	−1.45	−4.39	23.50	0.16	8.00	0.02
AREO 4 1890-94	1892	3.757	7.695	2.96	−1.41	−4.60	23.17	0.14	7.96	0.02
AREO 4 1895-99	1897	3.847	7.676	3.60	−1.69	−4.42	23.43	0.17	7.99	0.02
AREO 4 1900-04	1902	3.758	7.643	3.40	−1.61	−4.51	23.37	0.14	7.99	0.02
AREO 4 1905-09	1907	3.619	7.709	3.75	−1.65	−4.84	23.95	0.19	8.06	0.02
AREO 4 1910-14	1912	3.583	7.720	3.07	−1.95	−4.44	22.52	0.16	7.86	0.02
AREO 4 1915-19	1917	3.747	7.726	3.40	−1.26	−4.58	24.00	0.13	8.07	0.01
AREO 4 1920-24	1922	3.855	7.729	2.92	−1.59	−4.34	22.62	0.19	7.88	0.03
AREO 4 1925-29	1927	3.672	7.732	3.12	−1.90	−4.99	23.98	0.12	8.06	0.01
AREO 4 1930-34	1932	3.785	7.708	2.82	−2.15	−4.81	22.02	0.14	7.78	0.02
AREO 4 1935-39	1937	3.787	7.699	2.61	−1.63	−4.68	21.63	0.19	7.70	0.04
AREO 4-1940	1940	3.805	7.786	4.03	−1.77	−4.89	21.65	0.17	7.71	0.03
AREO 4-1941	1941	3.837	7.688	2.68	−1.44	−4.39	23.90	0.16	8.05	0.02
AREO 4-1942	1942	3.616	7.758	4.26	−1.37	−4.69	24.24	0.14	8.09	0.02
AREO 4-1943	1943	3.667	7.747	2.80	−1.85	−5.32	24.09	0.15	8.08	0.02
AREO 4-1944	1944	3.637	7.746	3.53	−1.40	−4.70	24.22	0.28	8.09	0.03
AREO 4-1945	1945	3.746	7.705	3.52	−1.91	−4.83	24.05	0.24	8.07	0.03
AREO 4-1946	1946	3.671	7.665	2.85	−1.28	−4.97	24.73	0.15	8.15	0.02
AREO 4-1947	1947	3.676	7.762	3.76	−1.64	−4.77	25.14	0.10	8.19	0.01
AREO 4-1948	1948	3.590	7.741	3.60	−1.74	−4.49	24.64	0.13	8.14	0.01
AREO 4-1949	1949	3.625	7.687	3.43	−1.72	−4.81	23.80	0.17	8.04	0.02
AREO 4-1950	1950	3.673	7.722	4.18	−1.65	−4.74	23.99	0.21	8.06	0.02
AREO 4-1951	1951	3.811	7.736	3.56	−1.54	−4.83	24.08	0.14	8.08	0.02
AREO 4-1952	1952	3.786	7.735	2.81	−1.69	−4.70	23.46	0.16	8.00	0.02
AREO 4-1953	1953	4.104	8.036	7.22	−2.12	−5.64	23.32	0.17	7.98	0.02
AREO 4-1954	1954	3.780	7.671	3.80	−1.75	−5.28	23.45	0.18	8.00	0.02

AREO 4-1955	1955	3.943	7.914	3.54	−1.44	−4.90	23.14	0.18	7.96	0.02
AREO 4-1956	1956	3.810	7.760	2.74	−1.62	−5.01	22.96	0.23	7.93	0.03
AREO 4-1957	1957	3.938	7.992	2.87	−1.86	−4.93	23.25	0.13	7.97	0.02
AREO 4-1958	1958	3.988	7.762	2.91	−1.79	−4.52	23.67	0.17	8.02	0.02
AREO 4-1959	1959	4.123	8.006	3.48	−1.77	−4.81	23.06	0.21	7.94	0.03
AREO 4-1960	1960	3.980	8.073	3.34	−1.64	−4.51	23.55	0.24	8.01	0.03
AREO 4-1961	1961	3.761	7.673	2.37	−1.83	−4.66	23.04	0.18	7.94	0.02
AREO 4-1962	1962	4.004	7.749	3.34	−1.73	−4.69	22.76	0.15	7.90	0.02
AREO 4-1963	1963	3.828	7.653	2.68	−1.86	−5.42	23.09	0.13	7.95	0.02
AREO 4-1964	1964	3.890	7.663	3.04	−1.78	−4.90	23.30	0.17	7.98	0.02
AREO 4-1965	1965	3.827	7.686	2.69	−1.83	−4.73	23.74	0.11	8.03	0.01
AREO 4-1966	1966	3.850	7.734	3.51	−1.92	−4.95	24.08	0.11	8.08	0.01
AREO 4-1967	1967	3.790	7.685	2.93	−1.68	−4.63	23.61	0.15	8.02	0.02
AREO 4-1968	1968	3.836	7.695	3.33	−1.81	−4.94	23.96	0.15	8.06	0.02
AREO 4-1969	1969	3.756	7.670	3.20	−1.76	−5.40	23.90	0.18	8.05	0.02
AREO 4-1970	1970	3.892	7.661	3.05	−1.77	−4.52	23.52	0.29	8.01	0.04
AREO 4-1971	1971	3.899	7.968	3.49	−1.65	−4.85	23.57	0.18	8.01	0.02
AREO 4-1972	1972	3.926	7.674	4.22	−2.00	−5.37	23.90	0.19	8.05	0.02
AREO 4-1973	1973	4.011	7.926	4.47	−1.72	−4.75	23.19	0.14	7.96	0.02
AREO 4-1974	1974	3.728	7.579	2.68	−1.71	−4.62	23.83	0.15	8.04	0.02
AREO 4-1975	1975	3.791	7.674	3.66	−1.96	−5.17	23.77	0.11	8.04	0.01
AREO 4-1976	1976	3.961	7.824	2.85	−1.76	−4.64	23.34	0.16	7.98	0.02
AREO 4-1977	1977	3.855	7.597	3.00	−2.23	−5.36	22.96	0.17	7.93	0.02
AREO 4-1978	1978	3.765	7.695	3.47	−2.25	−5.24	23.37	0.16	7.99	0.02
AREO 4-1979	1979	4.005	7.655	2.72	−1.87	−4.66	23.45	0.20	8.00	0.02
AREO 4-1980	1980	4.038	7.703	3.17	−2.10	−5.20	22.29	0.22	7.83	0.03
AREO 4-1981	1981	4.031	7.906	3.46	−1.94	−4.79	23.26	0.16	7.97	0.02
AREO 4-1982	1982	4.186	7.618	3.25	−1.85	−4.89	23.32	0.16	7.98	0.02
AREO 4-1983	1983	3.896	7.685	2.63	−1.72	−4.70	23.61	0.16	8.02	0.02
AREO 4-1984	1984	3.775	7.648	3.23	−1.96	−4.96	23.82	0.20	8.04	0.02
AREO 4-1985	1985	3.832	7.601	3.83	−2.28	−5.37	23.38	0.25	7.99	0.03
AREO 4-1986	1986	3.837	7.693	2.38	−2.46	−5.53	22.42	0.23	7.85	0.04
AREO 4-1987	1987	3.886	7.675	2.95	−2.35	−5.41	22.71	0.28	7.89	0.04
AREO 4-1988	1988	4.033	7.487	4.12	−2.77	−5.42	22.70	0.18	7.89	0.03
AREO 4-1989	1989	4.133	7.722	3.76	−3.08	−5.45	22.97	0.14	7.93	0.02
AREO 4-1990	1990	3.896	7.707	3.33	−2.60	−5.26	22.86	0.20	7.92	0.03
AREO 4-1991	1991	4.093	7.694	2.99	−2.22	−4.84	22.88	0.18	7.92	0.02
AREO 4-1992	1992	4.078	7.698	2.58	−2.89	−5.54	23.40	0.11	7.99	0.01
AREO 4-1993	1993	3.888	7.727	2.64	−2.55	−4.98	24.61	0.13	8.14	0.02
AREO 4-1994	1994	3.966	7.690	2.86	−2.42	−4.59	24.19	0.17	8.09	0.02
AREO 4-1995	1995	4.111	7.619	4.12	−2.50	−4.87	24.16	0.13	8.08	0.01
AREO 4-1996	1996	4.311	7.606	2.88	−2.75	−4.98	22.62	0.16	7.88	0.02
AREO 4-1997	1997	3.998	7.713	3.22	−2.65	−4.70	21.65	0.18	7.71	0.03

(*continued on next page*)

Table 2 (*continued*)

Sample ID	Year[a]	Mg/Ca^b ($\times10^{-3}$)	Sr/Ca^b ($\times10^{-3}$)	Ba/Ca^b ($\times10^{-6}$)	$\delta^{13}C^c$ (‰)	$\delta^{18}O^c$ (‰)	$\delta^{11}B^d$ (‰)	2σ	pH[e]	$2\sigma_{mean}$ [e]
AREO 4-1998	1998	4.351	7.610	2.92	−2.82	−5.21	21.06	0.21	7.57	0.05
AREO 4-1999	1999	4.061	7.722	3.60	−3.33	−4.80	21.97	0.20	7.77	0.03
AREO 4-2000	2000	4.120	7.628	3.48	−3.14	−5.29	22.22	0.14	7.81	0.02
AREO 4-2001	2001	4.160	7.653	3.46	−3.12	−4.97	21.93	0.16	7.76	0.03
AREO 4-2002	2002	4.238	7.663	3.10	−2.69	−5.32	23.82	0.16	8.04	0.02
AREO 4-2003	2003	4.196	7.752	4.40	−2.72	−5.96	23.74	0.16	8.03	0.02
AREO 4-2004	2004	4.108	7.691	22.16	−3.56	−5.25	21.45	0.28	7.66	0.05

[a] Samples from 1805 to 1939 are in 5-year interval, and the years for these samples are the average of the 5-year.
[b] Mg/Ca, Sr/Ca and Ba/Ca are molecular ratios.
[c] $\delta^{13}C$ and $\delta^{18}O$ are relative to Vienna PDB standard.
[d] $\delta^{11}B$ are relative to the long-term average of SRM 951 measured on this machine, 4.0532.
[e] pH values are calculated using the following parameters: $\alpha_{(B3-B4)} = 1.0204$ (Xiao et al., 2006), $pK_B = 8.60$ (Honisch et al., 2004) and seawater $\delta^{11}B = 40.08‰$ of our measurement for the GBR seawater.

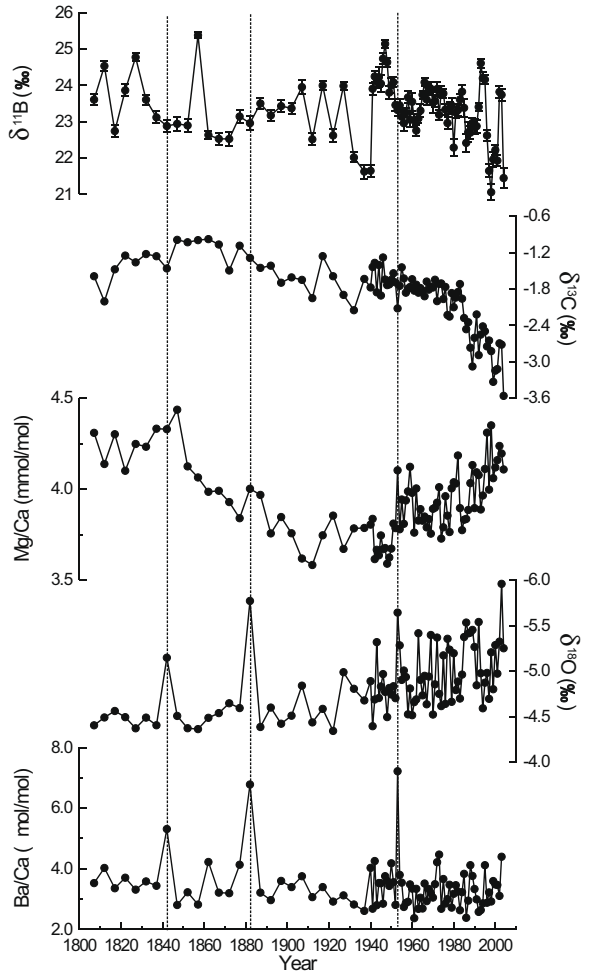

Fig. 4. Temporal variations of $\delta^{11}B$, $\delta^{13}C$, Mg/Ca, $\delta^{18}O$ and Ba/Ca ratios of the *Porites* coral from Arlington Reef. The vertical lines indicate the pronounced oscillations of $\delta^{18}O$ and Ba/Ca ratios around the year of 1840, 1880 and in 1953.

between the variations of coral $\delta^{11}B$ in the GBR and IPO index is unclear and as discussed below only partially accounts for the overall variability.

In addition to the interdecadal fluctuations, there is an overall decreasing trend in the Arlington Reef $\delta^{11}B$ record, particularly after 1940, when $\delta^{11}B$ varies from ~25‰ in 1947 to ~21‰ in 2004. This trend is not readily apparent in the Flinders Reef as it does not cover the time interval after 1990. The overall trend of decreasing $\delta^{11}B$ in the Arlington Reef record also corresponds to the more continuous trend to more negative of $\delta^{13}C$ values and the progressive increase of Mg/Ca ratios after 1940 (Fig. 4), where significant positive correlation, (coefficient of 0.62 with $n = 64$, $p < 0.0001$), exists between $\delta^{11}B$ and $\delta^{13}C$, and significant negative correlation, (coefficient of −0.60 with $n = 64$, $p < 0.0001$), occurs between $\delta^{11}B$ and Mg/Ca ratios (Fig. 7). Coral Mg/Ca is very sensitive to temperature change with higher Mg/Ca in coral skeleton corresponding to higher sea surface temperatures (SST) (Mitsuguchi et al., 1996). Even though biological/metabolic effect may influence Mg/Ca in coral skeleton (Mitsuguchi et al., 2003),

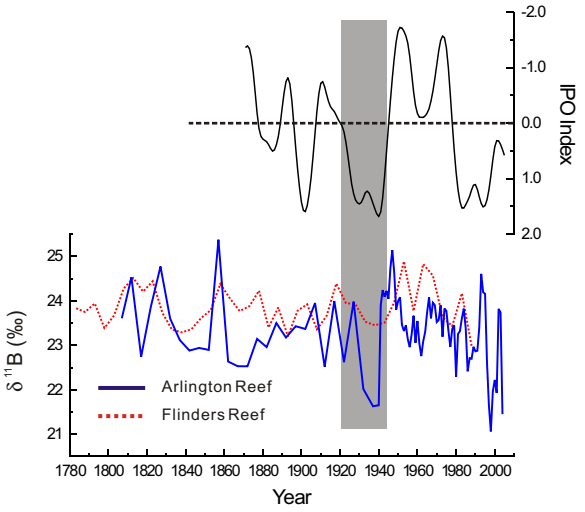

Fig. 5. Comparison between the $\delta^{11}B$ records of the *Porites* corals from Arlington Reef and Flinders Reef, and the IPO index. The $\delta^{11}B$ record from Flinders Reef is from Pelejero et al. (2005). The IPO index is the temperature anomaly of January-February-March (Folland et al., 1999). The shaded bar highlights the rapid change around 1940.

which hinder the utility of Mg/Ca to obtain precise SST records in old corals, the positive correlation between SST and Mg/Ca in modern corals is generally robust (Wei et al., 2000). In our coral records from Arlington Reef as shown in Fig. 4, the gradual increase of Mg/Ca since 1940 indicates continuously warming in this region, which agrees with the generally trend of global warming. The regional warming is also supported by the trend of more negative $\delta^{18}O$ values shown in Fig. 4. On the other hand, even though metabolic CO_2 within the polyps is believed to play a significant role in calcification of coral skeleton, the contribution of the DIC from external seawater remains an important factor (Al-Horani et al., 2003a). Thus, the long-term change of the coral $\delta^{13}C$ recorded in the Arlington coral is interpreted as reflecting the dissolved inorganic carbon (DIC) in the surface ocean. Therefore, the variation of coral $\delta^{11}B$ at Arlington Reef positively correlates with the on-going decrease of the $\delta^{13}C$ of DIC in seawater, and negatively correlates with the secular warming in this region after 1940.

As discussed, the $\delta^{11}B$ composition of coral skeletons records the pH in the ECF, the internal fluid where calcification occurs (Honisch et al., 2004), so the coral $\delta^{11}B$

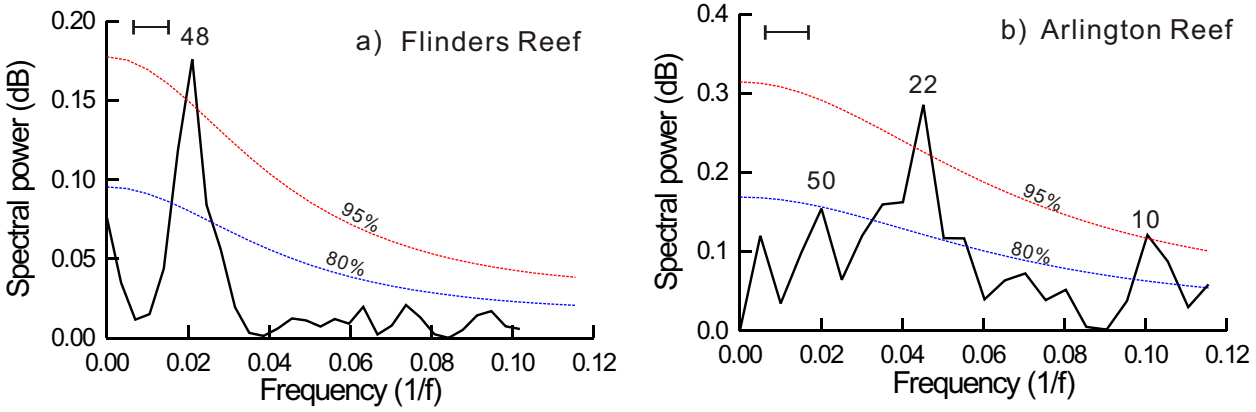

Fig. 6. Power spectra of the two pH records calculated using the software of REDFIT (Schulz and Mudelsee, 2002).(a) Record from Flinders Reef; (b) record from Arlington Reef. The horizontal bars indicate the bandwidths, and the dashed lines indicate the 95% and 80% confident levels.

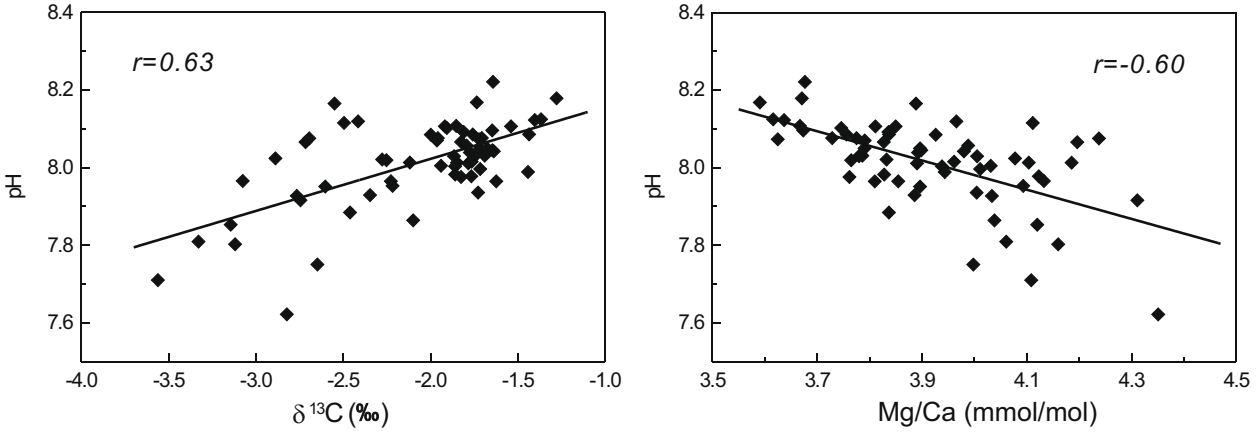

Fig. 7. Correlations between pH and $\delta^{13}C$ and Mg/Ca ratios of the *Porites* coral after 1940.

variation indicates the pH change in the ECF rather than that in ambient seawater. The mechanisms controlling the relationship between the pH in the ECF changes in ambient seawater pH remains uncertain, and clearly biological processes in coral polyps, such as photosynthesis and respiration, can obviously influence the ECF pH values (Al-Horani et al., 2003a). Thus, while the role of biological or 'vital effects' on coral $\delta^{11}B$ compositions cannot be ignored, coral culturing experiments under controlled conditions indicate that the variations of the $\delta^{11}B$ in coral skeleton actively response to the pH changes in ambient seawater. Corals generally exhibit a broadly similar relationship to that expected for the theoretical fractionation curve of $B(OH)_4^-$, but with systematic species dependent offsets (Honisch et al.,2004, 2007). Therefore, the variation of coral $\delta^{11}B$ appears to primarily reflect the pH changes in ambient seawater, even though more calibrations are required to convert coral $\delta^{11}B$ values into precise seawater pH values for seawater. In this respect, the interdecadal fluctuation of the coral $\delta^{11}B$ records in the GBR may indicate a response of seawater pH changes to the IPO, and the significant trend of decreasing $\delta^{11}B$ values in the Arlington Reef record after 1940 is consistent with a secular trend towards ocean acidification or decreasing seawater pH in this region.

The negative correlation between the SST and the coral $\delta^{11}B$ as shown in Fig. 7 shows a correlation between secular seawater acidification and warming since 1940. Increasing SST decreases the solubility of CO_2 in seawater and may therefore partially mitigate the trend of decreasing pH. Furthermore for corals operating below their thermal optimum, increasing temperature may enhance the photosynthesis of the *zooxanthella*, and thereby increase the pH in the ECF for calcification (Al-Horani et al., 2003a), as protons are consumed during photosynthesis (McConnaughey and Whelan, 1997). Thus, by itself increasing SST would tend to favor higher $\delta^{11}B$ in coral skeleton rather than the observed trend of decreasing $\delta^{11}B$ values. However, the observed negative correlation between the coral pH and the increasing SST (higher Mg/Ca) indicates that since 1940 temperature effects have been more than offset by the secular decrease of seawater pH from rapidly rising atmospheric CO_2. This is consistent with the model calculations of Cao et al. (2007) who show that increasing SST from climate change produces only second-order modifications to the ocean carbonate chemistry, with the main driver being increased CO_2 emissions.

The positive correlation between coral $\delta^{11}B$ and $\delta^{13}C$ shown in Fig. 7 indicates a correlation between seawater acidification and decreasing DIC $\delta^{13}C$ in this region since 1940. The trend of increasing negative DIC $\delta^{13}C$ in the past century is attributed to increasing anthropogenic emissions of CO_2 to the atmosphere with strongly negative $\delta^{13}C$ values from burning of fossil fuels (Bohm et al., 2002; Quay et al., 2003). Increasing anthropogenic emissions thus not only increases levels of atmospheric CO_2 concentration but also decreases the $\delta^{13}C$ composition of the atmosphere. Therefore, the positive correlation between coral pH and $\delta^{13}C$ records provides strong confirmation that the seawater acidification is closely linked to the anthropogenic CO_2 emissions from burning of fossil fuels.

4.2. Estimating the seawater pH changes from the coral $\delta^{11}B$ record

Assuming that the $\delta^{11}B$ in carbonates is representative of the $B(OH)_4^-$ in seawater, pH values can be calculated from the carbonate $\delta^{11}B$ using the following equation (e.g. Zeebe et al., 2001).

$$\mathrm{pH} = \mathrm{p}K_B - \log\left[\frac{\delta^{11}B_{SW} - \delta^{11}B_{Carbonate}}{\alpha_{B3-B4}\delta^{11}B_{Carbonate} - \delta^{11}B_{SW} + 1000(\alpha_{B3-B4} - 1)}\right]$$

The parameters in this equation are as follows: $\alpha_{(B3-B4)}$ (or $\alpha_{B(OH)_3-B(OH)_4^-}$ represents the fractionation factor for isotope exchange between $B(OH)_3$ and $B(OH)_4^-$ in seawater, pK_B the equilibrium constant for the dissociation of boric acid, and $\delta^{11}B_{SW}$ and $\delta^{11}B_{Carbonate}$ represent the $\delta^{11}B$ in seawater and in carbonate, respectively. Recognizing that the coral $\delta^{11}B$ records the pH in the ECF rather than that in the ambient seawater (Honisch et al., 2004), the empirical relation between coral $\delta^{11}B$ and seawater pH may have offsets from the theoretical equation. The pK_B (~8.6) and seawater $\delta^{11}B$ (~39.5‰) have been experimentally determined and relatively well constrained particularly for recent samples (Honisch et al., 2004). However, there is still considerable debate (Honisch et al., 2007), particularly on the appropriate value of $\alpha_{(B3-B4)}$, (Klochko et al., 2006; Zeebe, 2005) and Pagani et al. (2005) challenges the utility of boron isotope as seawater pH proxy on longer time-scales.

Currently, there are several possible $\alpha_{(B3-B4)}$ values. The theoretically $\alpha_{(B3-B4)}$, of ~1.0194 calculated at 25 °C, by (Kakihana et al., 1977) has generally been used in pH calculation (Honisch et al., 2004; Pelejero et al., 2005; Sanyal et al., 2001; Sanyal et al., 1996). However, most recent improved theoretical calculations give $\alpha_{(B3-B4)}$ values ranging from ~1.020 to ~1.030 at 25 °C (Klochko et al., 2006; Zeebe, 2005), with new experimental measurements suggesting an $\alpha_{(B3-B4)}$ in seawater at 25 °C of 1.0272 ± 0.0006 (Klochko et al., 2006). In a critical re-evaluation of the empirical data (Honisch et al., 2007) suggest that $\alpha_{(B3-B4)} = 1.020$ may best fit the empirical relationship between coral $\delta^{11}B$ and seawater pH. This value is similar to that suggested for *Porites* coral by Xiao et al. (2006), of 1.0204. It is important to note that the use of different $\alpha_{(B3-B4)}$ in calculating seawater pH from coral $\delta^{11}B$, effects not only the absolute pH values but also has a second-order effect on the differential changes in pH.

Table 3
Summary of pH calculated from $\delta^{11}B$ of the Arlington Reef coral using different $\alpha_{(B3-B4)}$.

$\alpha_{(B3-B4)}$	Maximum pH	Minimum pH	Amplitude	Grand mean
1.0194	8.20	7.46	0.74	7.94
1.0204	8.28	7.71	0.57	8.05
1.0272	8.58	8.29	0.29	8.45

The calculation assumes $pK_B = 8.59$ and seawater $\delta^{11}B = 39.5‰$.

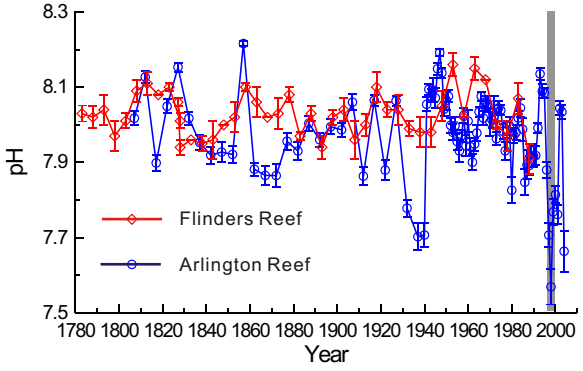

Fig. 8. pH estimations from the $\delta^{11}B$ records of the *Porites* corals from Arlington Reef and Flinders Reef. The shaded bar indicates the major bleaching event in the Great Barrier Reef during 1998.

In the absence of a detailed knowledge of how the physiological mechanisms of calcification and photosynthesis influence the boron isotopic composition of the carbonate skeleton (Honisch et al., 2004), calibrating $\delta^{11}B$ in coral skeleton using in-situ measured seawater pH values remains a priority. Unfortunately as noted by other authors (Zeebe, 2005) this has been inhibited by the lack of continuous in-situ measured pH records within coral reefs.

Recognizing these limitations Table 3 summaries the maximum, minimum, variation amplitude and grand mean of the coral pH values calculate using the different values of $\alpha_{(B3-B4)}$, assuming $pK_B = 8.59$ and seawater $\delta^{11}B = 39.5‰$. The calculated pH using $\alpha_{(B3-B4)} = 1.0272$, range from 8.58 to 8.29 with an average of 8.45; far too high compared with the average pH of modern seawater of 8.1 to 8.2. The pH calculated using $\alpha_{(B3-B4)} = 1.0194$ range from 8.20 to 7.46, with grand mean of 7.94. The minimum pH, 7.46, is clearly out of the range of the modern observed seawater pH in the west Pacific, of 7.7–8.2 (Honisch and Hemming, 2004), and the grand mean, 7.94, is lower than modern observations. The calculated pH using $\alpha_{(B3-B4)} = 1.0204$ is more reasonable giving a slightly higher range from 8.25 to 7.71, which are closer to modern observation, although the low values are still apparently anomalous.

Considering the uncertainties in both the Honisch et al. (2004, 2007) and Xiao et al. (2006) estimations, here we use an average value of 1.0204 for $\alpha_{(B3-B4)}$ consistent with the suggestion of Xiao et al. (2006) and seawater $\delta^{11}B = 40.08‰$, our measured value for the GBR seawater, in our calculation, and the calculated pH results are listed in Table 2, and shown in Fig. 8. The pH record in Flinders Reef is also shown in Fig. 8 for comparison. The $\delta^{11}B$-coral record of seawater pH in Arlington Reef appears to have changed significantly in the past 200 years, with a decreasing trend in pH from 8.22 in 1947 to 7.66 in 2004. This suggests an increasing trend towards acidification of seawater in Arlington Reef particularly during the last 60 years. Regardless of the pH calibration used, our coral $\delta^{11}B$ record also indicates abrupt changes in seawater pH variation amplitude particularly during the late 1940s and late 1990s of up to ~0.5 pH units. These rapid short-term oscillations are much larger than what can be attributed to regional changes in seawater pH, suggesting that other factors are influencing the coral $\delta^{11}B$ values as discussed in Section 4.3 below.

4.3. Vital effects versus local changes in the pH of coral reef waters

The much larger pH variation ranges in the Arlington Reef record compared to those in the Flinders Reef record appears to indicate that the change of seawater pH is spatially variable, and in particular the variation of seawater pH may be enlarged in the near-shore regions compared to regions away from shore.

Local changes in reef water pH at Arlington Reef may arise from low salinity flood-plumes since the runoff from eastern Australian rivers generally has a wide range of pH values, from >8.5 to <5 (Hatje et al., 2001; Sammut et al., 1996). With the increasing prevalence of acid soil runoff from disturbance of coastal mangrove systems the prevalence of low pH runoff in coastal regions has increased significantly (Lin and Melville, 1993; Sammut et al., 1996). Although Arlington Reef is a typical outer mid-shelf reef, it is relatively close to the coast and occasionally subject to the influence of flood-plumes generated by the monsoonal dominated river runoff. Flood-plume impacts can be constrained by the combined use of Ba/Ca and $\delta^{18}O$ compositions. Riverine fluxes to the Great Barrier Reef are generally characterized by high Ba contents due to desorption of Ba from suspended terrestrial sediments, and hence high Ba/Ca ratios in corals generally indicates terrestrial (sediment) inputs (Alibert et al., 2003; McCulloch et al., 2003). In addition the $\delta^{18}O$ composition of the river water is much lower than that of the seawater, and thus low salinity river flood-plumes are characterized by more negative $\delta^{18}O$ values in coral skeleton (McCulloch et al., 1994). There are three large Ba/Ca peaks occurring in 1840, 1880 and in 1953, accompanied by significant negative $\delta^{18}O$ peaks (Fig. 4). These are indicative of large river flood-plumes impacting to the central GBR during these periods. However, there is no $\delta^{11}B$ anomaly or significantly lower pH values associated with these events indicating that flood-plume activity has minimal effects on the pH of Arlington Reef. Also, the Ba/Ca variation shows no trend that is similar to that of the $\delta^{11}B$ after 1940. Therefore, terrestrial input to the GBR cannot account for the large decrease in reef water pH implied by the low $\delta^{11}B$ values.

An alternate and more feasible explanation of the short-term rapid oscillations in $\delta^{11}B$ values especially during the 1940 and 1998 periods is due to major changes in the physiological processes or vital effects controlling coral calcification. Recent experimental studies by (Al-Horani et al., 2003b) using micro-electrodes within the calcifying region (ie beneath the calicoblastic ectoderm) of the corals confirm that along with increasing the Ca ion concentration the pH is also increased. This increases the concentration of carbonate relative to bicarbonate ions and hence the degree of aragonite saturation, thereby promoting calcification. It is also likely that physiological processes associate with coral calcification will also modify the boron isotopic composition relative to that expected for the borate species in ambient seawater. Although the likely physiological control

or 'vital effect' on the B isotopic composition is not well understood, higher internal pH required for coral calcification may provide an explanation for the difference between the empirically observed B fraction of 1.020 versus the higher value of 1.0276 given by from direct estimates of $\alpha_{(B3-B4)}$.

Coral bleaching will significantly perturb calcification as a result of the loss of the *zooxanthella*. This is consistent with the observation in 1998 and in early 2002 of widespread coral bleaching in the GBR (Berkelmans et al., 2004), due to exceptionally warm temperatures. It is suggested that this caused via a major reduction of the internal pH at the sites of coral calcification hence reducing the skeletal $\delta^{11}B$ values. Thus, in addition to registering external changes in reef water pH, the coral $\delta^{11}B$ values maybe highly sensitive indicators of coral bleaching. If correct this would imply that a major coral bleaching event also occurred during the 1940s when the $\delta^{11}B$ values registered a decrease in pH to 7.75.

5. SUMMARY

In this paper, we report a long-term $\delta^{11}B$ variation record of a *Porites* coral from the Great Barriers Reef, together with other geochemical records that are closely to climatic and environmental changes, such as Mg/Ca, Ba/Ca ratios, and oxygen and carbon isotopes. These records cover the time span from 1800 to 2004 at 1 to 5-year time resolution. They provide details of changes seawater pH over the past 200 years in this region, and provide strong constraints on the processes driving changes in surface seawater pH. The main points of this study are as follows:

1) Positive TIMS method was adopted in this study to provide high-precision measurements of boron isotopic composition of modern corals. The internal precision and reproducibility for $\delta^{11}B$ of our measurements are all better than $\pm 0.2‰$ (2σ), providing an equivalent precision for pH estimations of generally better than ± 0.02.
2) The long-term variation of seawater pH derived from coral $\delta^{11}B$ record shows robust decadal–interdecadal cycles with periods of 22-year and 10-year over the past 200 years in this region. This suggests that the long-term seawater pH variation in this region is closely related to the decadal–interdecadal variability of atmospheric and oceanic anomalies in Pacific, which agrees with findings by Pelejero et al. (2005).
3) Coupled with this long-term variation, a significant acidification trend occurs from 1940s to present, with pH decrease of about 0.2-0.4, estimating using different $\alpha_{(B3-B4)}$ values. Comparisons with other paleoclimate proxies in particular $\delta^{13}C$ values, indicate that the trend towards ocean acidification over the past 60 years in this region is mostly the result of rapidly increasing of levels of atmospheric CO_2 contributed by human activities. This suggests that the increasing of anthropogenic CO_2 in atmosphere has caused significant acidification in the oceans in the past decades, especially in coastal regions and that the rate of ocean acidification is increasing.
4) The boron isotopic systematics in corals is also highly sensitive to perturbations in the physiological processes controlling coral calcification. In particular coral bleaching may have the effect of substantially reducing the pH beneath the calicoblastic ectoderm at the site of calcification. This results in a major reduction in the $\delta^{11}B$ composition of the resultant skeletal aragonite suggesting that in addition to recording ambient seawater pH conditions B isotopes are sensitive indicators of past bleaching events.

ACKNOWLEDGMENTS

The authors thanks to H. Scott-Gagan and J. Cowley of the Research School of Earth Sciences for their help in milling coral samples, and L. Kinsley for the help in mass spectrometry measurements. The constructive comments of the two anonymous reviewers and Dr. Julie Trotter helped to improve the manuscript. This work was supported by funding from ARC grant DP0559039 awarded to Malcolm McCulloch and support from the ARC Centre of Excellence for Coral Reef Studies. Gangjian Wei was supported by grants from the Chinese Academy of Sciences (Grant KZCX2-YW-318), the National Natural Science Foundation of China (Grant 40673075), and the Chinese Ministry of Science and Technology Special Scheme (Grant 2007CB815905). This is contribution No IS-1035 from GIGCAS.

REFERENCES

Al-Horani F. A., Al-Moghrabi S. M. and de Beer D. (2003a) The mechanism of calcification and its relation to photosynthesis and respiration in the scleractinian coral Galaxea fascicularis. *Mar. Biol.* **142**, 419–426.

Al-Horani F. A., Al-Moghrabi S. M. and de Beer D. (2003b) Microsensor study of photosynthesis and calcification in the scleractinian coral, Galaxea fascicularis: active internal carbon cycle. *J. Exp. Mar. Biol. Ecol.* **288**, 1–15.

Alibert C., Kinsley L., Fallon S. J., McCulloch M. T., Berkelmans R. and McAllister F. (2003) Source of trace element variability in Great Barrier Reef corals affected by the Burdekin flood plumes. *Geochim. Cosmochim. Acta* **67**, 231–246.

Berkelmans R., De'ath G., Kininmonth S. and Skirving W. J. (2004) A comparison of the 1998 and 2002 coral bleaching events on the Great Barrier Reef: spatial correlation, patterns, and predictions. *Coral Reefs* **23**, 74–83.

Bohm F., Haase-Schramm A., Eisenhauer A., Dullo W. C., Joachimski M. M., Lehnert H. and Reitner J. (2002) Evidence for preindustrial variations in the marine surface water carbonate system from coralline sponges. *Geochem. Geophys. Geosyst.* **3**, 1019. doi:10.1029/2001GC000264.

Caldeira K. and Wickett M. E. (2003) Anthropogenic carbon and ocean pH. *Nature* **425**, 365.

Cao L. and Caldeira K. (2008) Atmospheric CO_2 stabilization and ocean acidification. *Geophys. Res. Lett.* **35**, L19609. doi:10.1029/2008GL035072.

Cao L., Caldeira K. and Jain A. K. (2007) Effects of carbon dioxide and climate change on ocean acidification and carbonate mineral saturation. *Geophys. Res. Lett.* **34**, L05607. doi:10.1029/2006GL028605.

Cobb K. M., Charles C. D. and Hunter D. E. (2001) A central tropical Pacific coral demonstrates Pacific, Indian, and Atlantic decadal climate connections. *Geophys. Res. Lett.* **28**, 2209–2212.

Feely R. A., Sabine C. L., Lee K., Berelson W., Kleypas J., Fabry V. J. and Millero F. J. (2004) Impact of anthropogenic CO_2 on the $CaCO_3$ system in the oceans. *Science* **305**, 362–366.

Folland C. K., Parker D. E., Colman A. and Washington R. (1999) Large scale modes of ocean surface temperature since the late nineteenth century. In *Beyond El Nino: Decadal and Interdecadal Climate Variability* (ed. A. Navarra). Springer-Verlag, pp. 73–102.

Gattuso J. P., Allemand D. and Frankignoulle M. (1999) Photosynthesis and calcification at cellular, organismal and community levels in coral reefs: a review on interactions and control by carbonate chemistry. *Am. Zool.* **39**, 160–183.

Hatje V., Birch G. F. and Hill D. M. (2001) Spatial and temporal variability of particulate trace metals in Port Jackson Estuary, Australia. *Estuar. Coast. Shelf Sci.* **53**, 63–77.

Haugan P. M. and Drange H. (1996) Effects of CO_2 on the ocean environment. *Energ. Convers. Manage.* **37**, 1019–1022.

Hemming N. G. and Hanson G. N. (1992) Boron isotopic composition and concentration in modern marine carbonates. *Geochim. Cosmochim. Acta* **56**, 537–543.

Hemming N. G., Guilderson T. P. and Fairbanks R. G. (1998) Seasonal variations in the boron isotopic composition of coral: a productivity signal? *Global Biogeochem. Cy.* **12**, 581–586.

Hendy E. J., Gagan M. K., Alibert C. A., McCulloch M. T., Lough J. M. and Isdale P. J. (2002) Abrupt decrease in tropical Pacific Sea surface salinity at end of little ice age. *Science* **295**, 1511–1514.

Hershey J. P., Fernandez M., Milne P. J. and Millero F. J. (1986) The ionization of boric acid in NaCl, Na–Ca–Cl and Na–Mg–Cl solutions at 25 °C. *Geochim. Cosmochim. Acta* **50**, 143–148.

Hoegh-Guldberg O., Mumby P. J., Hooten A. J., Steneck R. S., Greenfield P., Gomez E., Harvell C. D., Sale P. F., Edwards A. J., Caldeira K., Knowlton N., Eakin C. M., Iglesias-Prieto R., Muthiga N., Bradbury R. H., Dubi A. and Hatziolos M. E. (2007) Coral reefs under rapid climate change and ocean acidification. *Science* **318**, 1737–1742.

Honisch B. and Hemming N. G. (2004) Ground-truthing the boron isotope-paleo-pH proxy in planktonic foraminifera shells: partial dissolution and shell size effects. *Paleoceanography* **19**, PA4010. doi:10.1029/2004PA001026.

Honisch B. and Hemming N. G. (2005) Surface ocean pH response to variations in pCO_2 through two full glacial cycles. *Earth Planet. Sci. Lett.* **236**, 305–314.

Honisch B., Hemming N. G., Grottoli A. G., Amat A., Hanson G. N. and Buma J. (2004) Assessing scleractinian corals as recorders for paleo-pH: empirical calibration and vital effects. *Geochim. Cosmochim. Acta* **68**, 3675–3685.

Honisch B., Hemming N. G. and Loose B. (2007) Comment on "A critical evaluation of the boron isotope-pH proxy: the accuracy of ancient ocean pH estimates" by M. Pagani, D. Lemarchand, A. Spivack and J. Gaillardet. *Geochim. Cosmochim. Acta* **71**, 1636–1641.

Intergovernmental Panel on Climate Changes (2007). Climate Change 2007: Synthesis Report. Contribution of Working Groups I, II and III *to the Fourth Assessment Report of the Intergovernmental Panel on Climate Change* (eds. Core Writing Team, R. K. Pachauri, and A. Reisinger). IPCC, Geneva, Switzerland. p. 104.

Kakihana H., Kotaka M., Satoh S., Nomura M. and Okamoto M. (1977) Fundamental studies on the ion-exchange separation of boron isotopes B. *Chem. Soc. Jpn.* **50**, 158–163.

Kleypas J. A., Buddemeier R. W., ArcherGattuso D., Gattuso J.-P., Langdon C. and Opdyke B. N. (1999) Geochemical consequences of increased atmospheric CO_2 on coral reefs. *Science* **284**, 118–120.

Klochko K., Kaufman A. J., Yao W. S., Byrne R. H. and Tossell J. A. (2006) Experimental measurement of boron isotope fractionation in seawater. *Earth Planet. Sci. Lett.* **248**, 276–285.

Kuhl M., Cohen Y., Dalsgaard T., Jorgensen B. B. and Revsbech N. P. (1995) Microenvironment and photosynthesis of zooxanthellae in scleractinian corals studied with microsensors for O_2, pH and light. *Mar. Ecol. Prog. Ser.* **117**, 159–172.

Langdon C. and Atkinson M. J. (2005) Effect of elevated pCO(2) on photosynthesis and calcification of corals and interactions with seasonal change in temperature/irradiance and nutrient enrichment. *Journal of Geophysical Research-Oceans* **110**, C09S07. doi:10.1029/2004JC002576.

Lemarchand D., Gaillardet J., Gopel C. and Manhes G. (2002) An optimized procedure for boron separation and mass spectrometry analysis for river samples. *Chem. Geol.* **182**, 323–334.

Lin C. and Melville M. D. (1993) Control of soil acidification by fluvial sedimentation in an estuarine floodplain, eastern Australia. *Sediment. Geol.* **85**, 271–284.

Linsley B. K., Wellington G. M. and Schrag D. P. (2000a) Decadal sea surface temperature variability in the subtropical South Pacific from 1726 to 1997 AD. *Science* **290**, 1145–1148.

Linsley R. K., Ren L., Dunbar R. B. and Howe S. S. (2000b) El Nino Southern Oscillation (ENSO) and decadal-scale climate variability at 10 N in the eastern Pacific from 1893 to 1994: a coral-based reconstruction from Clipperton Atoll. *Paleoceanography* **15**, 322–335.

Mantua N. J. and Hare S. R. (2002) The Pacific decadal oscillation. *J. Oceanogr.* **58**, 35–44.

McConnaughey T. A. and Whelan J. F. (1997) Calcification generates protons for nutrient and bicarbonate uptake. *Earth Sci. Rev.* **42**, 95–117.

McCulloch M. T., Gagan M. K., Mortimer G. E., Chivas A. R. and Isdale P. J. (1994) A high-resolution Sr/Ca and $\delta^{18}O$ coral record from the Great Barrier Reef, Australia, and the 1982–1983 El-Nino. *Geochim. Cosmochim. Acta* **58**, 2747–2754.

McCulloch M., Fallon S., Wyndham T., Hendy E., Lough J. and Barnes D. (2003) Coral record of increased sediment flux to the inner Great Barrier Reef since European settlement. *Nature* **421**, 727–730.

Miles H., Widdicombe S., Spicer J. I. and Hall-Spencer J. (2007) Effects of anthropogenic seawater acidification on acid-base balance in the sea urchin Psammechinus miliaris. *Mar. Poll. Bull.* **54**, 89–96.

Mitsuguchi T., Matsumoto E., Abe O., Uchida T. and Isdale P. J. (1996) Mg/Ca thermometry in coral skeletons. *Science* **274**, 961–963.

Mitsuguchi T., Matsumoto E. and Uchida T. (2003) Mg/Ca and Sr/Ca ratios of Porites coral skeleton: evaluation of the effect of skeletal growth rate. *Coral Reefs* **22**, 381–388.

Morse J. W., Andersson A. J. and Mackenzie F. T. (2006) Initial responses of carbonate-rich shelf sediments to rising atmospheric pCO_2 and "ocean acidification": role of high Mg-calcites. *Geochim. Cosmochim. Acta* **70**, 5814–5830.

Orr J. C., Maier-Reimer E., Mikolajewicz U., Monfray P., Sarmiento J. L., Toggweiler J. R., Taylor N. K., Palmer J., Gruber N., Sabine C. L., Le Quere C., Key R. M. and Boutin J. (2001) Estimates of anthropogenic carbon uptake from four three-dimensional global ocean models. *Global Biogeochem. Cy.* **15**, 43–60.

Orr J. C., Fabry V. J., Aumont O., Bopp L., Doney S. C., Feely R. A., Gnanadesikan A., Gruber N., Ishida A., Joos F., Key R. M., Lindsay K., Maier-Reimer E., Matear R., Monfray P., Mouchet A., Najjar R. G., Plattner G. K., Rodgers K. B., Sabine C. L., Sarmiento J. L., Schlitzer R., Slater R. D., Totterdell I. J., Weirig M. F., Yamanaka Y. and Yool A. (2005)

Anthropogenic ocean acidification over the twenty-first century and its impact on calcifying organisms. *Nature* **437**, 681–686.

Pagani M., Lemarchand D., Spivack A. and Gaillardet J. (2005) A critical evaluation of the boron isotope-pH proxy: the accuracy of ancient ocean pH estimates. *Geochim. Cosmochim. Acta* **69**, 953–961.

Pearson P. N. and Palmer M. R. (1999) Middle eocene seawater pH and atmospheric carbon dioxide concentrations. *Science* **284**, 1824–1826.

Pelejero C., Calvo E., McCulloch M. T., Marshall J. F., Gagan M. K., Lough J. M. and Opdyke B. N. (2005) Preindustrial to modern interdecadal variability in coral reef pH. *Science* **309**, 2204–2207.

Power S., Casey T., Folland C., Colman A. and Mehta V. (1999) Inter-decadal modulation of the impact of ENSO on Australia. *Clim. Dynam.* **15**, 319–324.

Quay P., Sonnerup R., Westby T., Stutsman J. and McNichol A. (2003) Changes in the $^{13}C/^{12}C$ of dissolved inorganic carbon in the ocean as a tracer of anthropogenic CO_2 uptake. *Global Biogeochem. Cy.* **17**, 1004. doi:10.1029/2001GB001817.

Roberts J. M., Wheeler A. J. and Freiwald A. (2006) Reefs of the deep: the biology and geology of cold-water coral ecosystems. *Science* **312**, 543–547.

Sammut J., White I. and Melville M. D. (1996) Acidification of an estuarine tributary in eastern Australia due to drainage of acid sulfate soils. *Mar. Freshw. Res.* **47**, 669–684.

Sanyal A., Hemming N. G., Hanson G. N. and Broecker W. S. (1995) Evidence for a higher pH in the glacial ocean from boron isotopes in foraminifera. *Nature* **373**, 234–236.

Sanyal A., Hemming N. G., Broecker W. S., Lea D. W., Spero H. J. and Hanson G. N. (1996) Oceanic pH control on the boron isotopic composition of foraminifera: evidence from culture experiments. *Paleoceanography* **11**, 513–517.

Sanyal A., Hemming N. G., Broecker W. S. and Hanson G. N. (1997) Changes in pH in the eastern equatorial Pacific across stage 5–6 boundary based on boron isotopes in foraminifera. *Global Biogeochem. Cy.* **11**, 125–133.

Sanyal A., Bijma J., Spero H. and Lea D. W. (2001) Empirical relationship between pH and the boron isotopic composition of Globigerinoides sacculifer: implications for the boron isotope paleo-pH proxy. *Paleoceanography* **16**, 515–519.

Schulz M. and Mudelsee M. (2002) REDFIT: estimating red-noise spectra directly from unevenly spaced paleoclimatic time series. *Comput. Geosci.* **28**, 421–426.

Spivack A. J. and Edmond J. M. (1986) Determination of boron isotope ratios by thermal ionization mass spectrometry of the dicesium metaborate cation. *Anal. Chem.* **58**, 31–35.

Sun Y. L., Sun M., Wei G. J., Lee T., Nie B. F. and Yu Z. W. (2004) Strontium contents of a Porites coral from Xisha Island, South China Sea: a proxy for sea-surface temperature of the 20th century. *Paleoceanography* **19**, PA2004. doi:10.1029/2003PA000959.

Vengosh A., Kolodny Y., Starinsky A., Chivas A. R. and Mcculloch M. T. (1991) Coprecipitation and isotopic fractionation of boron in modern biogenic carbonates. *Geochim. Cosmochim. Acta* **55**, 2901–2910.

Wei G. J., Sun M., Li X. H. and Nie B. F. (2000) Mg/Ca, Sr/Ca and U/Ca ratios of a porites coral from Sanya Bay, Hainan Island, South China Sea and their relationships to sea surface temperature. *Palaeogeogr. Palaeoclimatol. Palaeoecol.* **162**, 59–74.

Wei G. J., Deng W. F., Yu K. F., Li X. H., Sun W. D. and Zhao J. X. (2007) Sea surface temperature records in the northern South China Sea from mid-Holocene coral Sr/Ca ratios. *Paleoceanography* **22**, PA3206. doi:10.1029/2006PA001270.

Wei H. Z., Xiao Y. K., Sun A., Zhang C. G. and Li S. Z. (2004) Effective elimination of isobaric ions interference and precise thermal ionization mass spectrometer analysis for boron isotope. *Int. J. Mass Spectrom.* **235**, 187–195.

Xiao Y. K., Beary E. S. and Fassett J. D. (1988) An improved method for the high-precision isotopic measurement of boron by thermal ionization mass spectrometry Int. *J. Mass Spectrom. Ion Proc.* **85**, 203–213.

Xiao Y. K., Shirodkar P. V., Zhang C. G., Wei H. Z., Liu W. G. and Zhou W. J. (2006) Isotopic fractionation of boron in growing corals and its palaeoenvironmental implication. *Curr. Sci.* **90**, 414–420.

Zeebe R. E. (2005) Stable boron isotope fractionation between dissolved $B(OH)_3$ and $B(OH)_4^-$. *Geochim. Cosmochim. Acta* **69**, 2753–2766.

Zeebe R. E., Sanyal A., Ortiz J. D. and Wolf-Gladrow D. A. (2001) A theoretical study of the kinetics of the boric acid-borate equilibrium in seawater. *Mar. Chem.* **73**, 113–124.

Associate editor: Anne Cohen